A Quasi-Static Boundary Value Problem in Multi-Surface Elastoplasticity: Part 2 – Numerical Solution

Martin Brokate *, Carsten Carstensen †, Jan Valdman ‡

Abstract

Multi-yield elastoplasticity models a material with more then one plastic state and hence allows for refined approximation of irreversible deformations. Aspects of the mathematical modeling and a proof of unique existence of weak solutions can be found in part I of this paper [BCV04]. In this part II we establish a canonical time-space discretization of the evolution problem and present various algorithms for the solving really discrete problems. Based on a global Newton-Raphson solver, we carefully study and solve elementwise inner iterations. Numerical examples illustrate the model and its flexibility to allow for refined hysteresis curves.

Keywords Variational inequalities, elastoplasticity, phase transition multi-surface model, multi-yield Prandtl-Ishlinskii model, hysteresis, finite element method
AMS Subject Classification 47J40, 49J40, 74C05.

1 Introduction

In this article we consider the quasi-static initial-boundary value problem for small strain elastoplasticity with a multi-surface constitutive law of linear kinematic hardening type. In the first part [BCV04], we presented the precise formulation of the initial-boundary value problem in the form of a system of evolution variational inequalities for unknown fields of displacement and several plastic strain components attached to different surfaces. We proved the existence and uniqueness of its solution by verifying the assumptions of a general theorem [HR99] and also derived an estimate for the ellipticity constant in dependence on the material parameters.

This second part concerns a time-space discretization of the system of variational inequalities presented in the first part, it develops a solution algorithm and reports

*Zentrum Mathematik, TU Munich, Boltzmannstrasse 3, D-85747 Garching, Germany, e-mail: brokate@ma.tum.de

†Department of Mathematics, Humboldt Universität zu Berlin, Unter den Linden 6, D-10099 Berlin, Germany, e-mail: cc@math.hu-berlin.de

‡Special Research Program SFB F013 'Numerical and Symbolic Scientific Computing', Johannes Kepler University Linz, Altenbergerstrasse 69, A-4040 Linz, Austria, e-mail: Jan.Valdman@sfb013.uni-linz.ac.at

on numerical examples in 2D and 3D. For the numerical treatment of single-yield hardening models described by a single variational inequality we refer to [AC00]. In those works, we use the conforming finite element space of lowest order with elementwise linear displacement and constant plastic strains. In order to describe the multi-yield aspect in a compact way, a matrix formulation is used and original system of inequalities is rewritten as an equilibrium equality and an elementwise matrix inequality for plastic strains only. Then, an algorithm with an outer Newton-Raphson method for solving the equilibrium equality is applied. An inner loop for elementwise solution of the matrix inequality is carefully studied. It has already been shown that a solution of the elementwise inequality can be written explicitly in the single-yield case. Our analysis indicates that, already in the two-yield case, the situation is considerably more difficult. Indeed, one encounters root finding of a system of two polynomials that can be reduced to an 8-th degree polynomial symbolically. Alternatively, we derive an iterative algorithm for the original matrix inequality and prove its convergence with the rate 1/2.

Numerical experiments demonstrate the feasibility of the algorithm; the different hysteresis behavior curves and elastoplastic zones and their evolution is shown. An illustrating movie for a time-evolving elastoplastic process can be downloaded from the web [ani].

The paper is organized as follows. Section 2 briefly recalls the mathematical formulation from part I and then establishes the discrete model. The Newton-Raphson method of Section 3 allows for an effective solution of the nonlinear system of variational equations with an outer and an elementwise inner loop. Numerical examples in Section 4 illustrate the behavior of the proposed refined two-yield elastoplastic model.

2 Mathematical Model and its Discretization

Following the first part of this article [BCV04] the multi-yield elastoplastic continuum can be modeled by the following evolution variational inequality:

Problem 2.1 (BVP of quasi-static multi-surface elastoplasticity). *Given $\ell \in H^1(0,T;\mathcal{H}^*)$ with $\ell(0)=0$ in a Hilbert space $\mathcal{H}$ and its dual $\mathcal{H}^*$ and duality bracket $\langle\cdot,\cdot\rangle$, find $x \in H^1(0,T;\mathcal{H})$ with $x(0)=0$ such that*

$$\langle \ell(t), y-\dot{x}(t)\rangle \le a(x(t), y-\dot{x}(t)) + \psi(y) - \psi(\dot{x}(t)) \quad \text{for all } y \in \mathcal{H}. \tag{1}$$

holds for almost all $t \in (0,T)$.

Therein, we are given $x=(u,(p_r)_{r\in I}), y=(v,(q_r)_{r\in I})$ belonging to the space $\mathcal{H} = H^1_D(\Omega) \times \prod_{r\in I} \operatorname{dev}(L^2(\Omega)^{d\times d}_{\text{sym}})$ with

$$H^1_D(\Omega) = \{v \in H^1(\Omega)^d | v=0 \text{ on } \Gamma_D\},$$
$$\operatorname{dev}(L^2(\Omega)^{d\times d}_{\text{sym}}) = \{q \in L^2(\Omega)^{d\times d}: \text{ for all } x\in\Omega, q(x) \in \operatorname{dev}\mathbb{R}^{d\times d}_{\text{sym}}\},$$

for the usual Sobolev and Lebesgue spaces $H^1(\Omega)$ and $L^2(\Omega)$, $\operatorname{dev}\mathbb{R}^{d\times d}_{\text{sym}}$ is defined using the deviatoric operator $\operatorname{dev}: \mathbb{R}^{d\times d}_{\text{sym}} \to \mathbb{R}^{d\times d}_{\text{sym}}, \operatorname{dev} q = q - \frac{1}{d}\operatorname{tr} q\mathbb{I}$ by

$$\operatorname{dev}\mathbb{R}^{d\times d}_{\text{sym}} = \{q \in \mathbb{R}^{d\times d}_{\text{sym}} : \exists p \in \mathbb{R}^{d\times d}_{\text{sym}}, q = \operatorname{dev} p\}.$$

Here and below, $\mathbb{I}$ denotes the identity tensor (an identity matrix) and $\operatorname{tr} : \mathbb{R}^{d\times d} \to \mathbb{R}$ defines the trace of a matrix, $\operatorname{tr}\varepsilon := \sum_{j=1}^{d} \varepsilon_{jj}$, for $\varepsilon \in \mathbb{R}^{d\times d}_{\mathrm{sym}}$, where d is the problem dimension. The bilinear form $a(\cdot,\cdot)$, the linear form $\ell(t)$, and the nonlinear functional ψ read

$$\begin{aligned}
a : \mathcal{H} \times \mathcal{H} \to \mathbb{R}, \quad & a(x,y) = \int_\Omega \mathbb{C}(\varepsilon(u) - \sum_{r\in I} p_r) : (\varepsilon(v) - \sum_{r\in I} q_r)\,\mathrm{d}x \\
& \qquad + \sum_{r\in I} \int_\Omega \mathbb{H}_r p_r : q_r \,\mathrm{d}x, \\
\ell(t) : \mathcal{H} \to \mathbb{R}, \quad & \langle \ell(t), y \rangle = \int_\Omega f(t)\cdot v\,\mathrm{d}x + \int_{\Gamma_N} g(t)\cdot v\,\mathrm{d}S(x), \\
\psi : \mathcal{H} \to \mathbb{R}, \quad & \psi(y) = \sum_{r\in I} \int_\Omega \sigma_r^y |q_r|\,\mathrm{d}x.
\end{aligned} \tag{2}$$

The linear elasticity matrix $\mathbb{C}$ from the isotropic case is defined by

$$\mathbb{C}\varepsilon = 2\mu\varepsilon + \lambda(\operatorname{tr}\varepsilon)\mathbb{I},$$

for the (positive) Lamé coefficients μ and λ. The hardening matrices read $\mathbb{H}_r = h_r\mathbb{I}$, where $h_r > 0$ are hardening coefficients. According to the choice of the index set I we classify a single-yield case with $I = \{1\}$, a two-yield case with $I = \{1, 2\}$ and a more general M-yield case with $I = \{1, \dots, M\}$.

The discretization of the variational inequality (1) consists of time and space discretizations. We discretize the continuous time interval $(0, T)$ by the discrete times $t_0, \dots, t_N$ with

$$0 = t_0 < \tau_1 \le t_1 < \tau_2 \le t_2 < \cdots \le t_{N-1} < \tau_N \le t_N = T,$$

with a time step $k_j = t_j - t_{j-1}, j = 1, \dots, N$ and the polygonal domain $\Omega \subset \mathbb{R}^2$ by a regular triangulation $\mathcal{T}$ in triangles in sense of Ciarlet [Cia78], i.e. $\mathcal{T}$ is a finite partition of Ω into closed triangles; two distinct elements T_1 and T_2 are either disjoint, or $T_1 \cap T_2$ is a complete edge or a common node of both T_1 and T_2. In the first time step t_1, the time derivative $\dot{x}(t_1)$ is approximated by the backward Euler method as $\dot{X}^1 = \frac{X^1 - X^0}{k_1}$. The Hilbert space $\mathcal{H}$ is approximated by the conforming finite element subspace

$$\mathcal{S} = \mathcal{S}^1_D(\mathcal{T}) \times \prod_{r\in I} \operatorname{dev}(\mathcal{S}^0(\mathcal{T})^{d\times d}_{\mathrm{sym}}),$$

which is a product space of the space of $\mathcal{T}$- piecewise constant functions

$$\operatorname{dev}(\mathcal{S}^0(\mathcal{T})^{d\times d}_{\mathrm{sym}}) := \{a \in L^2(\Omega)^{d\times d} : \forall T \in \mathcal{T}, a|_T \in \operatorname{dev}\mathbb{R}^{d\times d}_{\mathrm{sym}}\}$$

and the set of $\mathcal{T}$- piecewise affine functions that are zero on Γ_D by

$$\mathcal{S}^1_D(\mathcal{T}) := \{v \in H^1_D(\Omega) : \forall T \in \mathcal{T}, v|_T \in \mathcal{P}_1(T)^d\}.$$

($\mathcal{P}_1(T)$ denotes the affine functions on T.) We discretize the variational inequality (1) as follows. Find $X^1 = (U^1, (P_r^1)_{r\in I}) := (U^1, P^1) \in \mathcal{S}$ such that, for all $Y = (V, (Q_r)_{r\in I}) := (V, Q) \in \mathcal{S}$,

$$\langle \ell(t_1), (Y - \frac{X^1 - X^0}{k_1})\rangle \leq a(X^1, Y - \frac{X^1 - X^0}{k_1}) + \psi(Q) - \psi(\frac{P^1 - P^0}{k_1}).$$

After introducing an incremental variable $X := (U, P) = X^1 - X^0$ and a linear functional $L(Y) = \langle \ell(t_1), Y\rangle - a(X^0, Y)$ we obtain a one-time step discrete problem.

Lemma 1 (Equivalent Reformulations). *For each $X = (U, P) \in \mathcal{S}$ the following three conditions (a)-(c) are equivalent:*

$$\begin{array}{ll}
(a) & L(Y - X) \leq a(X, Y - X) + \psi(Y) - \psi(X) \quad \textit{for all } Y = (V, Q) \in \mathcal{S}. \\
(b) & \Phi(X) = \min\limits_{Y\in S} \Phi(Y) \quad \textit{for } \Phi(Y) = \dfrac{1}{2}a(Y, Y) + \psi(Q) - L(Y). \\
(c) & L(Y - X) = a(X, Y - X) \quad \textit{for all } Y = (V, P) \in \mathcal{S} \quad \textit{and} \\
 & L(Y - X) \leq a(X, Y - X) + \psi(Y) - \psi(X) \quad \textit{for all } Y = (U, Q) \in \mathcal{S}.
\end{array}$$

Proof. Elementary calculations with the quadratic forms, we omit the details. $\square$

The following matrix notation allows for a brief formulation of the discrete problem. Let

$$P := \begin{pmatrix} P_1 \\ \vdots \\ P_M \end{pmatrix}, P^0 := \begin{pmatrix} P_1^0 \\ \vdots \\ P_M^0 \end{pmatrix}, Q := \begin{pmatrix} Q_1 \\ \vdots \\ Q_M \end{pmatrix}, \hat{\Sigma} := \begin{pmatrix} \mathbb{C}\varepsilon(U) \\ \vdots \\ \mathbb{C}\varepsilon(U) \end{pmatrix},$$

$$\hat{\Sigma}^0 := \begin{pmatrix} \mathbb{C}\varepsilon(U^0) \\ \vdots \\ \mathbb{C}\varepsilon(U^0) \end{pmatrix}, \hat{\mathbb{C}} := \begin{pmatrix} \mathbb{C} & \dots & \mathbb{C} \\ \vdots & & \vdots \\ \mathbb{C} & \dots & \mathbb{C} \end{pmatrix}, \quad \hat{\mathbb{H}} := \begin{pmatrix} \mathbb{H}_1 & \dots & 0 \\ \vdots & & \vdots \\ 0 & \dots & \mathbb{H}_M \end{pmatrix}.$$

Since the plastic yield parameters $\sigma_1^y, \dots, \sigma_M^y$ are positive, the expansion

$$|(P_1, \dots, P_M)^T|_{\sigma^y} := \sigma_1^y|P_1| + \dots + \sigma_M^y|P_M|$$

defines a norm in $\mathbb{R}^{Md\times d}$. Then there holds

$$\begin{aligned}
-a(X, Y - X) &= \int_\Omega \Big(\Sigma - (\hat{\mathbb{C}} + \hat{\mathbb{H}})P\Big) : (Q - P)\,\mathrm{d}x, \\
L(Y - X) &= \int_\Omega \Big(\Sigma^0 - (\hat{\mathbb{C}} + \hat{\mathbb{H}})P^0\Big) : (Q - P)\,\mathrm{d}x, \\
\psi(Y) &= \int_\Omega |Q|_{\sigma^y}\,\mathrm{d}x.
\end{aligned}$$

With the substitution $\hat{A} := \hat{\Sigma} + \hat{\Sigma}^0 - (\hat{\mathbb{C}} + \hat{\mathbb{H}})P^0$, inequality (c) from Lemma 1 reads

$$\int_\Omega (\hat{A} - (\hat{\mathbb{C}} + \hat{\mathbb{H}})P) : (Q - P)\,\mathrm{d}x \leq \int_\Omega (|Q|_{\sigma^y} - |P|_{\sigma^y})\,\mathrm{d}x \tag{3}$$

for all $Q \in \prod_{r=1}^{M} \operatorname{dev}(\mathcal{S}^0(\mathcal{T})^{d\times d}_{\mathrm{sym}})$. Owing to the lowest order discretization, P and $\hat{A}$ are constant matrices on every triangle T of the triangulation $\mathcal{T}$. It enables us to decompose the inequality (3) elementwise. Given $\hat{A}, \hat{\mathbb{C}}, \hat{\mathbb{H}} \in \mathbb{R}^{Md\times Md}$, we seek $P = (P_1, \ldots, P_M)^T \in \mathbb{R}^{Md\times d}$ with $P_1, \ldots, P_M \in \operatorname{dev}\mathbb{R}^{d\times d}_{\mathrm{sym}}$, such that for all $Q = (Q_1, \ldots, Q_M)^T \in \mathbb{R}^{Md\times d}$ with $Q_1, \ldots, Q_M \in \operatorname{dev}\mathbb{R}^{d\times d}_{\mathrm{sym}}$ holds

$$(\hat{A} - (\hat{\mathbb{C}} + \hat{\mathbb{H}})P) : (Q - P) \leq |Q|_{\sigma^y} - |P|_{\sigma^y}. \tag{4}$$

Detailed formulation of the equilibrium equality together with the latter inequality define the discrete problem:

Problem 2.2 (Discrete problem). *Given* $U^0 \in \mathcal{S}^1_D(\mathcal{T}), P^0_1, \ldots, P^0_M \in \operatorname{dev}(\mathcal{S}^0(\mathcal{T})^{d\times d}_{sym})$, *seek* $U^1 \in \mathcal{S}^1_D(\mathcal{T})$ *such that for all* $V \in S^1_D(\mathcal{T})$,

$$\int_\Omega \mathbb{C}(\varepsilon(U^1) - \sum_{r=1}^{M} P^1_r) : \varepsilon(V)\, dx - \int_\Omega f(t)V\, dx - \int_{\Gamma_N} gV\, dx = 0. \tag{5}$$

Here $P = (P_1, \ldots, P_M)^T = (P^1_1, \ldots, P^1_M)^T - (P^0_1, \ldots, P^0_M)^T$ *satisfies elementwise the inequality*

$$(\hat{A} - (\hat{\mathbb{C}} + \hat{\mathbb{H}})P) : (Q - P) \leq |Q|_{\sigma^y} - |P|_{\sigma^y}.$$

3 Numerical solution of discrete model

The numerical solution of the discrete problem is discussed in this and the subsequent section for it is split into an outer and an inner iteration.

3.1 Outer Loop in Newton-Raphson scheme

For the triangulation $\mathcal{T}$ with N nodes, the equilibrium equality (5) represents a nonlinear system of $2N$ equations for $\mathbf{U^1} = (U^1_1, \ldots, U^1_{2N})^T$,

$$\mathbf{F}_i(\mathbf{U^1}) = 0 \quad \text{for all} \quad i = 1, \ldots, 2N. \tag{6}$$

We use the Newton-Raphson method for the iterative solution of (6).

Algorithm 3.1 (Newton-Raphson Method). *(a) Choose an initial approximation* $\mathbf{U^1_0} \in \mathbb{R}^{\mathbf{2N}}$, *set* $k := 0$.
(b) Let $k := k+1$, *solve* $\mathbf{U^1_k}$ *from* $D\mathbf{F}(\mathbf{U^1_{k-1}})(\mathbf{U^1_k} - \mathbf{U^1_{k-1}}) = -\mathbf{F}(\mathbf{U^1_{k-1}})$.
(c) If $\mathbf{U^1_k} - \mathbf{U^1_{k-1}}$ *is sufficiently small then output* $\mathbf{U^1_k}$, *otherwise goto (b).*

Remark 1. In order to incorporate the Dirichlet boundary conditions properly, the linear system in the step (b) is extended,

$$\begin{pmatrix} D\mathbf{F}(\mathbf{U^1_{k-1}}) & B^T \\ B & 0 \end{pmatrix} \begin{pmatrix} \mathbf{U^1_k} - \mathbf{U^1_{k-1}} \\ \lambda \end{pmatrix} = \begin{pmatrix} -\mathbf{F}(\mathbf{U^1_{k-1}}) \\ \mathbf{0} \end{pmatrix},$$

with some matrix B and the vector of Lagrange parameters λ, see [ACFK02].

Remark 2. Here, $D\mathbf{F}(\mathbf{U_k^1}) \in \mathbb{R}^{2N\times 2N}$ represents a sparse tangential stiffness matrix

$$D\mathbf{F}(\mathbf{U})_{ij} \approx \frac{\mathbf{F}(U_1,\dots,U_j+\epsilon_j,\dots,U_{2N})_i - \mathbf{F}(U_1,\dots,U_j-\epsilon_j,\dots,U_{2N})_i}{2\epsilon_j}$$

approximated by a central difference scheme with small parameters $\epsilon_j > 0$, $j = 1,\dots,2N$.

Remark 3 *(Three stages convergence control).* The termination criterion used in the step (c) reads

$$\frac{|\mathbf{U_k^1} - \mathbf{U_{k-1}^1}|}{|\mathbf{U_k^1}| + |\mathbf{U_{k-1}^1}|} < tol \quad \text{or} \quad |\mathbf{U_k^1}| + |\mathbf{U_{k-1}^1}| = 0$$

together with the condition $r_\mathbf{k} \geq r_\mathbf{k-1}$, where $r_\mathbf{k} = |\mathbf{F}(\mathbf{U_k^1}) - B^T\lambda|$ is a residual. If the number k of iterations exceeds some predefined bound, Algorithm 3.1 terminates with no solution.

Remark 4 *(Nested iterations).* The nested iteration technique [Hac85] is applied for the solution of the problem on nested meshes $\mathcal{T}_0 \subseteq T_1 \cdots \subseteq T_F$.

3.2 Inner loop for single-yield model

The single-yield model is specified by one plastic strain $P \in \mathbb{R}^{d\times d}_{\mathrm{sym}}$ with $\operatorname{tr} P = 0$, the elastic matrix $\mathbb{C}$ with $\mathbb{C}P = 2\mu P$, the hardening matrix $\mathbb{H}$ with $\mathbb{H}P = hP$, the matrix norm $|P|_{\sigma^y} = \sigma^y|P|$ and the matrix $A := \mathbb{C}\varepsilon(U) + \mathbb{C}\varepsilon(U^0) - (\mathbb{C}+\mathbb{H})P^0$.

Lemma 2 ([ACZ99]). *Given $A \in \mathbb{R}^{d\times d}_{sym}$ and $\sigma^y > 0$ there exists exactly one $P \in \operatorname{dev}\mathbb{R}^{d\times d}_{sym}$ that satisfies*

$$\{A - (\mathbb{C}+\mathbb{H})P\} : (Q-P) \leq \sigma^y\{|Q| - |P|\}$$

for all $Q \in \operatorname{dev}\mathbb{R}^{d\times d}_{sym}$. This P is characterized as the minimizer of

$$\frac{1}{2}(\mathbb{C}+\mathbb{H})Q : Q - Q : A + \sigma^y|Q| \tag{7}$$

(amongst trace-free symmetric $d\times d$-matrices) and is given by

$$P = \frac{(|\operatorname{dev} A| - \sigma^y)_+}{2\mu + h}\frac{\operatorname{dev} A}{|\operatorname{dev} A|}, \tag{8}$$

where $(\cdot)_+ := \max\{0,\cdot\}$ denotes the non-negative part. The minimal value of (7) (attained for P as in (8)) is

$$-\frac{1}{2}(|\operatorname{dev} A| - \sigma^y)_+^2/(2\mu+h).$$

3.3 Inner loop for two-yield model

The two-yield model is specified by two plastic strains P_1, P_2 that are coupled in a generalized plastic strain $P = (P_1, P_2)^T$. The generalized elasticity matrix and the generalized hardening matrices read

$$\hat{\mathbb{C}} := \begin{pmatrix} \mathbb{C} & \mathbb{C} \\ \mathbb{C} & \mathbb{C} \end{pmatrix} \quad \text{and} \quad \hat{\mathbb{H}} := \begin{pmatrix} \mathbb{H}_1 & 0 \\ 0 & \mathbb{H}_2 \end{pmatrix},$$

the generalized loading matrix reads

$$\hat{A} = \begin{pmatrix} A_1 \\ A_2 \end{pmatrix} = \begin{pmatrix} \mathbb{C}\varepsilon(U) \\ \mathbb{C}\varepsilon(U) \end{pmatrix} + \begin{pmatrix} \mathbb{C}\varepsilon(U^0) \\ \mathbb{C}\varepsilon(U^0) \end{pmatrix} - \begin{pmatrix} \mathbb{C} + \mathbb{H}_1 & \mathbb{C} \\ \mathbb{C} & \mathbb{C} + \mathbb{H}_2 \end{pmatrix} \begin{pmatrix} P_1^0 \\ P_2^0 \end{pmatrix}$$

and the matrix norm is defined by

$$|P|_{\sigma^y} = \sigma_1^y |P_1| + \sigma_2^y |P_2|.$$

Lemma 3. *Given $\hat{A} = (A_1, A_2)^T, A_1, A_2 \in \mathbb{R}^{d\times d}_{sym}$ there exists exactly one $P = (P_1, P_2)^T, P_1, P_2 \in \operatorname{dev} \mathbb{R}^{d\times d}_{sym}$ that satisfies*

$$(\hat{A} - (\hat{\mathbb{C}} + \hat{\mathbb{H}})P) : (Q - P) \leq |Q|_{\sigma^y} - |P|_{\sigma^y} \tag{9}$$

for all $Q = (Q_1, Q_2)^T, Q_1, Q_2 \in \operatorname{dev} \mathbb{R}^{d\times d}_{sym}$ This P is characterized as the minimizer of

$$f(Q) = \frac{1}{2}(\hat{\mathbb{C}} + \hat{\mathbb{H}})Q : Q - Q : \hat{A} + |Q|_{\sigma^y} \tag{10}$$

(amongst trace-free symmetric $d \times d$ matrices Q_1, Q_2).

Proof. The equivalence of $f(P) = \min_Q f(Q)$ and (9) is obvious. The function $f(Q)$ is strictly convex, continuous in the space of all trace-free symmetric d×d matrices Q_1, Q_2. There holds $\lim_{|Q|\to\infty} f(Q) = +\infty$, and so it attains exactly one minimum. □

Remark 5. In the absence of the off-diagonal blocks in the matrix $\hat{\mathbb{C}} = \operatorname{diag}(\mathbb{C}, \mathbb{C})$, the minimization problem (10) is separated into two independent minimization problems in P_1 and P_2. The solution reads

$$P_j = (\frac{(|\operatorname{dev} A_j| - \sigma_j^y)_+}{2\mu + h_j} \frac{\operatorname{dev} A_j}{|\operatorname{dev} A_j|} \quad \text{for } j = 1, 2.$$

3.4 Reduction to polynomial of degree 8 for two-yield model

In general, the elementwise inner loop leads to the computation of roots of a single non-linear equation.

Lemma 4. *Let B be a unit ball at the point 0, $B := \{Q \in \mathbb{R}^{d\times d}_{sym} : |Q| \leq 1\}$. Then the subdifferential of $|P|_{\sigma^y} = \sigma_1^y P_1 + \sigma_2^y P_2$, where $P = (P_1, P_2) \in \mathbb{R}^{d\times d} \times \mathbb{R}^{d\times d}$ has the following form*

$$\partial |\cdot|_{\sigma^y}(P) = \begin{cases} \sigma_1^y B \times \sigma_2^y B & \text{if } \; P_1 = P_2 = 0, \\ \{\sigma_1^y \frac{P_1}{|P_1|}\} \times \sigma_2^y B & \text{if } \; P_1 \neq 0, P_2 = 0, \\ \sigma_1^y B \times \{\sigma_2^y \frac{P_2}{|P_2|}\} & \text{if } \; P_1 = 0, P_2 \neq 0, \\ \{\sigma_1^y \frac{P_1}{|P_1|}\} \times \{\sigma_2^y \frac{P_2}{|P_2|}\} & \text{if } \; P_1 \neq 0, P_2 \neq 0. \end{cases}$$

Proof. By the definition, the convex function $|P|_{\sigma^y}$ is decomposed as two convex functions $\sigma_1^y|P_1|$ and $\sigma_2^y|P_2|$. Both functions have subdifferentials, namely

$$\partial(\sigma_1^y|P_1|)(P) = \begin{cases} \sigma_2^y B \times \{0\} & \text{if} \quad P_1 = 0, \\ \{\sigma_2^y \frac{P_2}{|P_2|}\} \times \{0\} & \text{if} \quad P_1 \neq 0 \end{cases} \tag{11}$$

and

$$\partial(\sigma_2^y|P_2|)(P) = \begin{cases} \{0\} \times \sigma_1^y B & \text{if} \quad P_2 = 0, \\ \{0\} \times \{\sigma_2^y \frac{P_2}{|P_2|}\} & \text{if} \quad P_2 \neq 0. \end{cases} \tag{12}$$

The convex functions $\sigma_1^y|P_1|$ and $\sigma_2^y|P_2|$, considered as functions of two variables P_1, P_2, are continuous at the point $P_1 = P_2 = 0$ in the space $\mathbb{R}^{d\times d}_{\text{sym}} \times \mathbb{R}^{d\times d}_{\text{sym}}$. Therefore, according to the calculus of convex analysis, we can write

$$\partial(|P|_{\sigma^y}) = \partial(\sigma_1^y|P_1|) + \partial(\sigma_2^y|P_2|).$$

The combination of (11) and (12) concludes the proof. $\square$

Lemma 4 divides the analysis of the inclusion

$$\begin{pmatrix} \operatorname{dev} A_1 \\ \operatorname{dev} A_2 \end{pmatrix} - \begin{pmatrix} (2\mu + h_1)\mathbb{I} & 2\mu\mathbb{I} \\ 2\mu\mathbb{I} & (2\mu + h_2)\mathbb{I} \end{pmatrix} \begin{pmatrix} P_1 \\ P_2 \end{pmatrix} \in (\partial|\cdot|_{\sigma^y}(P_1, P_2))^T$$

into four cases in dependence of the combination of the values of P_1 and P_2:

Case 1: $P_1 = P_2 = 0$ with the following equivalences

$$P_1 = P_2 = 0 \Leftrightarrow \quad |\operatorname{dev} A_1| \leq \sigma_1^y \text{ and } |\operatorname{dev} A_2| \leq \sigma_2^y.$$

Case 2: $P_1 = 0, P_2 \neq 0$, which means

$$\begin{pmatrix} \operatorname{dev} A_1 \\ \operatorname{dev} A_2 \end{pmatrix} - \begin{pmatrix} (2\mu + h_1)\mathbb{I} & 2\mu\mathbb{I} \\ 2\mu\mathbb{I} & (2\mu + h_2)\mathbb{I} \end{pmatrix} \begin{pmatrix} 0 \\ P_2 \end{pmatrix} \in \begin{pmatrix} \sigma_1^y B \\ \{\sigma_2^y \frac{P_2}{|P_2|}\} \end{pmatrix}.$$

We may write equivalently

$$\operatorname{dev} A_1 - 2\mu P_2 \in \sigma_1^y B, \tag{13}$$

$$\operatorname{dev} A_2 - (2\mu + h_2)P_2 = \sigma_2^y \frac{P_2}{|P_2|}. \tag{14}$$

Elimination of P_2 from (14) yields

$$P_2 = \frac{|\operatorname{dev} A_1| - \sigma_2^y}{2\mu + h_2} \frac{\operatorname{dev} A_2}{|\operatorname{dev} A_2|}$$

and the substitution of this into (13) finally gives the condition

$$\operatorname{dev} A_1 - 2\mu(\frac{|\operatorname{dev} A_1| - \sigma_2^y}{2\mu + h_2} \frac{\operatorname{dev} A_2}{|\operatorname{dev} A_2|}) \in \sigma_1^y B.$$

Case 3: $P_1 \neq 0, P_2 = 0$. The same technique as in Case 2., only with the reversed indices 1 and 2, gives

$$P_1 = \frac{|\operatorname{dev} A_2| - \sigma_1^y}{2\mu + h_1} \frac{\operatorname{dev} A_1}{|\operatorname{dev} A_1|},$$

$$\operatorname{dev} A_2 - 2\mu\left(\frac{|\operatorname{dev} A_2| - \sigma_1^y}{2\mu + h_1}\frac{\operatorname{dev} A_1}{|\operatorname{dev} A_1|}\right) \in \sigma_2^y B.$$

Case 4: $P_1 \neq 0, P_2 \neq 0$ implies

$$\begin{pmatrix}\operatorname{dev} A_1\\ \operatorname{dev} A_2\end{pmatrix} - \begin{pmatrix}(2\mu + h_1)\mathbb{I} & 2\mu\mathbb{I}\\ 2\mu\mathbb{I} & (2\mu + h_2)\mathbb{I}\end{pmatrix}\begin{pmatrix}P_1\\ P_2\end{pmatrix} = \begin{pmatrix}\sigma_1^y \frac{P_1}{|P_1|}\\ \sigma_2^y \frac{P_2}{|P_2|}\end{pmatrix}. \tag{15}$$

Applying substitutions $P_i = \xi_i X_i$, where $|X_i| = 1, i = 1, 2$, (15) becomes a system of nonlinear equations with positive parameters $\xi_1 = |P_1|, \xi_2 = |P_2|$, namely

$$\begin{pmatrix}\operatorname{dev} A_1\\ \operatorname{dev} A_2\end{pmatrix} = \begin{pmatrix}(\sigma_1^y + (2\mu + h_1)\xi_1)\mathbb{I} & 2\mu\xi_2\mathbb{I}\\ 2\mu\xi_1\mathbb{I} & (\sigma_2^y + (2\mu + h_2)\xi_2)\mathbb{I}\end{pmatrix}\begin{pmatrix}X_1\\ X_2\end{pmatrix}.$$

Additional substitutions $\eta_1 := \sigma_1^y + (2\mu + h_1)\xi_1, \eta_2 := \sigma_2^y + (2\mu + h_2)\xi_2, \nu_1 := 2\mu\xi_1, \nu_2 := 2\mu\xi_2$ and the fact that

$$\begin{pmatrix}\eta_1\mathbb{I} & \nu_2\mathbb{I}\\ \nu_1\mathbb{I} & \eta_2\mathbb{I}\end{pmatrix}^{-1} = \frac{1}{\eta_1\eta_2 - \nu_1\nu_2}\begin{pmatrix}\eta_2\mathbb{I} & -\nu_2\mathbb{I}\\ -\nu_1\mathbb{I} & \eta_1\mathbb{I}\end{pmatrix}$$

yield

$$\begin{aligned}\eta_2 \operatorname{dev} A_1 - \nu_2 \operatorname{dev} A_2 &= (\eta_1\eta_2 - \nu_1\nu_2)X_1,\\ -\nu_1 \operatorname{dev} A_1 + \eta_1 \operatorname{dev} A_2 &= (\eta_1\eta_2 - \nu_1\nu_2)X_2.\end{aligned} \tag{16}$$

Normalization of (16) and the application of substitutions for $\eta_1, \eta_2, \nu_1, \nu_2$ give the system of nonlinear equations for positive ξ_1, ξ_2

$$|l_1(\xi_1)| - |r(\xi_1, \xi_2)| = 0, \quad |l_2(\xi_2)| - |r(\xi_1, \xi_2)| = 0, \tag{17}$$

where

$$\begin{aligned}l_1(\xi_1) &= (\sigma_1^y + (2\mu + h_1)\xi_1) \operatorname{dev} A_2 - 2\mu\xi_1 \operatorname{dev} A_1,\\ l_2(\xi_2) &= (\sigma_2^y + (2\mu + h_2)\xi_2) \operatorname{dev} A_1 - 2\mu\xi_2 \operatorname{dev} A_2,\\ r(\xi_1, \xi_2) &= (\sigma_1^y + (2\mu + h_2)\xi_1)(\sigma_2^y + (2\mu + h_2)\xi_2) - 4\mu^2\xi_1\xi_2.\end{aligned}$$

Instead of the solving (17) we prefer to solve the equivalent system of nonlinear equations

$$\Phi_j(\xi_1, \xi_2) = |l_j(\xi_j)|^2 - (r(\xi_1, \xi_2))^2 = 0, \quad \text{for } j = 1, 2. \tag{18}$$

Lemma 5. *Given $\sigma_1^y, \sigma_2^y, h_1, h_2, \mu, \operatorname{dev} A_1, \operatorname{dev} A_2$. Then the solution ξ_2 of the nonlinear system (18) is a root of the 8-th degree polynomial of the form*

$$\begin{aligned}&\Big(J^4F^2\Big)\xi_2^8 + \Big(2T_4J^2F\Big)\xi_2^7 + \Big(2T_3J^2F + T_4^2\Big)\xi_2^6 + \Big(2T_2J^2F + 2T_3T_4\Big)\xi_2^5\\ &+\Big(2T_1J^2F + 2T_2T_4 + T_3^2 - F(BJ + 2IC)^2\Big)\xi_2^4\\ &+\Big(-E(BJ + 2IC)^2 - 2F(2CG + BH)(BJ + 2IC) + 2T_1T_4 + 2T_2T_3\Big)\xi_2^3\\ &+\Big(-D(BJ + 2IC)^2 - 2E(2CG + BH)(BJ + 2IC) - F(2CG + BH)^2\\ &\quad + 2T_1T_3 + T_2^2\Big)\xi_2^2\\ &+\Big(-2D(2CG+BH)(BJ+2IC) - E(2CG + BH)^2 + 2T_1T_2\Big)\xi_2\\ &+\Big(T_1^2 - D(2CG + BH)^2\Big) = 0,\end{aligned}$$

with the coefficients $A, B, C, D, E, F, G, H, I, J$ below and

$$
\begin{aligned}
T_1 &:= H^2\,\mathrm{D} - C\,G^2 - A\,H^2 - B\,G\,H - C\,D,\\
T_2 &:= -B\,G\,J - 2\,H\,J\,A - C\,E - 2\,I\,C\,G + H^2\,E - I\,B\,H + 2\,H\,J\,\mathrm{D},\\
T_3 &:= -C\,F - J^2\,A + 2\,H\,J\,E - I\,B\,J + C + J^2\,\mathrm{D} + H^2\,F,\\
T_4 &:= 2\,H\,J\,F + J^2\,E.
\end{aligned}
$$

Then

$$\xi_1 = \frac{-I\,\xi_2 - G \pm \sqrt{\mathrm{D} + E\,\xi_2 + F\,\xi_2^2}}{H + J\,\xi_2}.$$

Proof. Direct calculations reveal

$$
\begin{aligned}
|l_1(\xi_1)|^2 =& |((2\mu + h_1)\,\mathrm{dev}\,A_2 - 2\mu\,\mathrm{dev}\,A_1)\xi_1 + \sigma_1^y\,\mathrm{dev}\,A_2|^2\\
=& |\sigma_1^y\,\mathrm{dev}\,A_2|^2 + 2(\sigma_1^y\,\mathrm{dev}\,A_2) : ((2\mu + h_1)\,\mathrm{dev}\,A_2 - 2\mu\,\mathrm{dev}\,A_1)\xi_1\\
&+ |(2\mu + h_1)\,\mathrm{dev}\,A_2 - 2\mu\,\mathrm{dev}\,A_1|^2\xi_1^2 := A + B\xi_1 + C\xi_1^2,\\
|l_2(\xi_2)|^2 =& |((2\mu + h_2)\,\mathrm{dev}\,A_1 - 2\mu\,\mathrm{dev}\,A_2)\xi_2 + \sigma_2^y\,\mathrm{dev}\,A_1|^2\\
=& |\sigma_2^y\,\mathrm{dev}\,A_1|^2 + 2(\sigma_2^y\,\mathrm{dev}\,A_1) : ((2\mu + h_2)\,\mathrm{dev}\,A_1 - 2\mu\,\mathrm{dev}\,A_2)\xi_2\\
&+ |((2\mu + h_2)\,\mathrm{dev}\,A_1 - 2\mu\,\mathrm{dev}\,A_2)|^2\xi_2^2 := D + E\xi_2 + F\xi_2^2,\\
r(\xi_1, \xi_2)^2 =& (\sigma_1^y\sigma_2^y + (2\mu + h_1)\sigma_2^y\xi_1 + (2\mu + h_2)\sigma_1^y\xi_2 + (2\mu(h_1 + h_2) + h_1h_2)\xi_1\xi_2)^2\\
=& (G + H\xi_1 + I\xi_2 + J\xi_1\xi_2)^2.
\end{aligned}
$$

Then Φ_1, Φ_2 are polynomials of the second degree in two variables ξ_1, ξ_2:

$$
\begin{aligned}
\Phi_1(\xi_1, \xi_2) &= A + B\xi_1 + C\xi_1^2 - (G + H\xi_1 + I\xi_2 + J\xi_1\xi_2)^2 = 0\\
\Phi_2(\xi_1, \xi_2) &= D + E\xi_2 + F\xi_2^2 - (G + H\xi_1 + I\xi_2 + J\xi_1\xi_2)^2 = 0
\end{aligned}
$$

Expressing ξ_1 from the latter equation and a substitution into the former leads (with MAPLE 5) to the polynomial (5). □

Example 3.1. Let $\mu = 1, \sigma_1^y = 1, \sigma_2^y = 2, h_1 = 1, h_2 = 1$ and $A_1 = A_2 = \begin{pmatrix} 20 & 0 \\ 0 & 0 \end{pmatrix}$. The direct calculation shows

$$
\begin{aligned}
l_1(\xi_1) &= \begin{pmatrix} 10 + 10\xi_1 & 0 \\ 0 & -10 - 10\xi_1 \end{pmatrix},\\
l_2(\xi_2) &= \begin{pmatrix} 20 + 10\xi_2 & 0 \\ 0 & -20 - 10\xi_2 \end{pmatrix},\\
r(\xi_1, \xi_2) &= 5\,\xi_1\,\xi_2 + 6\,\xi_1 + 3\,\xi_2 + 2
\end{aligned}
$$

and the nonlinear system of equations (18) for positive $\xi_1, \xi_2 > 0$ reads

$$\Phi_1(\xi_1, \xi_2) = 200 + 400\,\xi_1 + 200\,\xi_1^2 - (2 + 3\,\xi_2 + 6\,\xi_1 + 5\,\xi_1\,\xi_2)^2 = 0, \tag{19}$$

$$\Phi_2(\xi_1, \xi_2) = 800 + 800\,\xi_2 + 200\,\xi_2^2 - (2 + 3\,\xi_2 + 6\,\xi_1 + 5\,\xi_1\,\xi_2)^2 = 0. \tag{20}$$

The unknown ξ_1 is expressed from (20)

$$\xi_1 = \frac{-3\xi_2 - 2 \pm 10\sqrt{10}(2 + \xi_2)}{5\xi_2 + 6}$$

and the substitution of the plus term into (19) implies after the factorization the equality

$$\frac{(5\xi_2 + 8 - 10\sqrt{2})(5\xi_2 + 4 - 10\sqrt{2})(\xi_2 + 2)^2}{(6 + 5\,\xi_2)} = 0. \tag{21}$$

Note that the substitution of the minus term (3.1) into (19) leads to the different signs of ξ_1 and ξ_2. The roots of (21) are given by

$$\xi_2 = \{-\frac{4}{5} + 2\sqrt{2}, -\frac{8}{5} - 2\sqrt{2}, -2, -2\}$$

There is one positive root $\xi_2 = -\frac{4}{5} + 2\sqrt{2} \approx 2.028427124$ only, whose substitution into (19) represents the quadratic equation $(995\xi_1 + 801 - 50\sqrt{2})(5\xi_1 - 1 - 10\sqrt{2}) = 0$ with roots

$$\xi_1 = \{-\frac{1}{5}\frac{-1 + 40\sqrt{2}}{1 + 10\sqrt{2}}, \frac{1}{5}\frac{201 + 2\sqrt{2}}{1 + 10\sqrt{2}}\}.$$

Merely the first root $\xi_1 = -\frac{1}{5}\frac{-1+40\sqrt{2}}{1+10\sqrt{2}} \approx 3.028427125$ is positive.

3.5 Iterative solution of the discrete inequality

The following iterative scheme is shown to converge towards the solution of the discrete inequality for the two-yield model.

Algorithm 3.2 (Iterative approach for calculation of P_1, P_2). *Input* $\mu, h_1, h_2, \sigma_1^y, \sigma_2^y$, $\operatorname{dev} A_1, \operatorname{dev} A_2$ *and tol* ≥ 0.
(a) Choose an initial approximation $(P_1^0, P_2^0) \in \operatorname{dev}\mathbb{R}^{d\times d}_{sym} \times \operatorname{dev}\mathbb{R}^{d\times d}_{sym}$*, set* $i := 0$.
(b) Find $P_2^{i+1} \in \operatorname{dev}\mathbb{R}^{d\times d}_{sym}$ *such that*

$$f(P_1^i, P_2^{i+1}) = \min_{Q \in dev\mathbb{R}^{d\times d}_{sym}} f(P_1^i, Q).$$

(c) Find $P_1^{i+1} \in \operatorname{dev}\mathbb{R}^{d\times d}_{sym}$ *such that*

$$f(P_1^{i+1}, P_2^{i+1}) = \min_{Q \in dev\mathbb{R}^{d\times d}_{sym}} f(Q, P_2^{i+1}).$$

(d) If $\frac{|P_1^{i+1} - P_1^i| + |P_2^{i+1} - P_2^i|}{|P_1^{i+1}| + |P_1^i| + |P_2^{i+1}| + |P_2^i|} > tol$ *set* $i := i + 1$ *and goto (b), otherwise output* (P_1^{i+1}, P_2^{i+1}).

Algorithm 3.2 belongs to the class of alternating direction algorithms. Similarly as in the single-yield case, the minimization problems in steps (b) and (c) can be solved explicitly as

$$\begin{aligned} P_2^{i+1} &= \frac{(|\operatorname{dev} A_2 - 2\mu P_1^i| - \sigma_2^y)_+}{2\mu + h_2}\frac{\operatorname{dev} A_2 - 2\mu P_1^i}{|\operatorname{dev} A_2 - 2\mu P_1^i|}, \\ P_1^{i+1} &= \frac{(|\operatorname{dev} A_1 - 2\mu P_2^{i+1}| - \sigma_1^y)_+}{2\mu + h_1}\frac{\operatorname{dev} A_1 - 2\mu P_2^{i+1}}{|\operatorname{dev} A_1 - 2\mu P_2^{i+1}|}. \end{aligned}$$

Proposition 1 states that Algorithm 3.2 converges with the convergence rate 1/2.

Proposition 1 (Convergence of Algorithm 3.2). *Let (P_1, P_2) be the minimizer of f and let the sequence $(P_1^i, P_2^i)_{i=0}^{\infty}$ be generated by Algorithm 3.2. Define $q := \gamma/(1+\gamma), \gamma := L^2 \cdot \alpha^{-2}, C_0 := 2(1+\gamma) \cdot \alpha^{-1} \cdot (f(P_1^0, P_2^0) - f(P_1, P_2))$, where $\alpha > 0$ and $L > 0$. Then, for any $i \geq 1$ there holds*

$$|P_1^i - P_1|^2 + |P_2^i - P_2|^2 \leq C_0\, q^i.$$

Proof. Let us decompose the space of $X := \operatorname{dev}(\mathbb{R}^{d\times d}_{\text{sym}}) \times \operatorname{dev}(\mathbb{R}^{d\times d}_{\text{sym}})$ as $X = X_1 + X_2$,

$$X_1 := \{(P_1, 0) : P_1 \in \operatorname{dev}(\mathbb{R}^{d\times d}_{\text{sym}})\} \quad \text{and} \quad X_2 := \{(0, P_2) : P_2 \in \operatorname{dev}(\mathbb{R}^{d\times d}_{\text{sym}})\}.$$

Let $M_1 : X \to X_1$ and $M_2 : X \to X_2$ be linear mappings defined as

$$M_1(P_1, P_2) := (P_1, 0) \quad \text{and} \quad M_2(P_1, P_2) := (0, P_2).$$

Then we can show that for all subsets $\Lambda \subseteq \{1, 2\}$ and all $P = (P_1, P_2) \in X$ there holds

$$|\sum_{\lambda\in\Lambda} M_\lambda(P_1, P_2)| \leq |(P_1, P_2)|.$$

We decompose the functional f as the sum of functionals Φ and ψ, where

$$\Phi(P) := \frac{1}{2}(\hat{\mathbb{H}} + \hat{\mathbb{C}})P : P - A : P \quad \text{and} \quad \psi(P) := |P|_{\sigma^y} = \sigma_1^y|P_1| + \sigma_2^y|P_2|.$$

One can show that the functional Φ is Fréchet-differentiable and $D\Phi$ is uniformly elliptic with a constant $\alpha > 0$ and Lipschitz continuous with a constant $L > 0$. The convex, lower-semicontinuous functional ψ is additive with respect to the partition $X = X_1 + X_2$, i.e. in the sense that, for all $(x_1, x_2) \in X_1 \times X_2$,

$$\psi(x_1 + x_2) = \psi(x_1) + \psi(x_2).$$

For all $j \in \{1, 2\}$, for all $y_j \in \sum_{k=1,k\neq j}^{2} X_k$, there holds $M_j y_j = 0$ and therefore for all $x_j \in X_j$ holds

$$\psi(x_j + M_j y_j) = \psi(x_j),$$

thus ψ is also independent with respect to the partition $X = X_1 + X_2$. Estimate (1) is then an immediate consequence of Theorem 2.1 in [Car97]. □

The next example illustrates the behavior of Algorithm 3.2.

Example 3.2. Let $\mu = 1, \sigma_1^y = 1, \sigma_2^y = 2, h_1 = 1, h_2 = 1, A_1 = A_2 = \begin{pmatrix} 20 & 0 \\ 0 & 0 \end{pmatrix}$, $tol = 10^{-12}$ and the initial approximation

$$P_2^0 = \frac{(|\operatorname{dev} A_2| - \sigma_2^y)_+}{2\mu + h_2} \frac{\operatorname{dev} A_2}{|\operatorname{dev} A_2|},\; P_1^0 = \frac{(|\operatorname{dev} A_1 - 2\mu P_2^0| - \sigma_1^y)_+}{2\mu + h_1} \frac{\operatorname{dev} A_1 - 2\mu P_2^0}{|\operatorname{dev} A_1 - 2\mu P_2^0|}.$$

Algorithm 3.2 generates approximations $P_1^i, P_2^i, i = 1, 2, \ldots$ in the form

$$P_1^i = \begin{pmatrix} x^i & 0 \\ 0 & -x^i \end{pmatrix} \quad \text{and} \quad P_2^i = \begin{pmatrix} y^i & 0 \\ 0 & -y^i \end{pmatrix},$$

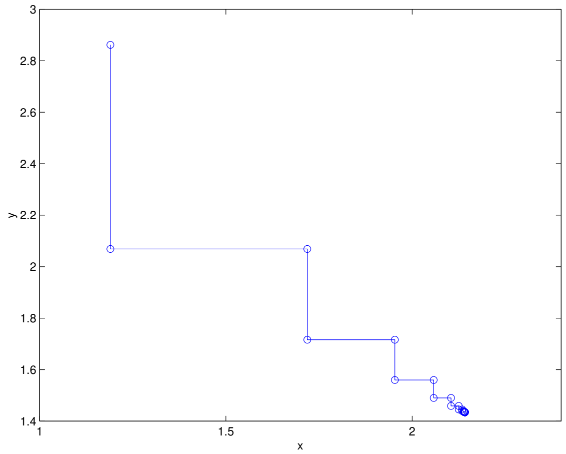

Figure 1: The approximations $P_1^i = (x^i, 0; 0, -x^i)$, $P_2^i = (y^i, 0; 0, -y^i)$, $i = 0, \ldots, 34$ computed by Algorithm 3.2 in Example 3.2 and displayed as the points (x^i, y^i) in the $x - y$ coordinate system.

and terminates after 34 approximations with

$$P_1^{34} = \begin{pmatrix} 2.14142 & 0 \\ 0 & -2.14142 \end{pmatrix} \quad \text{and} \quad P_2^{34} = \begin{pmatrix} 1.43431 & 0 \\ 0 & -1.4343 \end{pmatrix}.$$

Figure 1 displays the approximations $(P_1^i, P_2^i), i = 0, 1, 2, \ldots, 34$ as the points (x^i, y^i) in the $x - y$ coordinate system. Note that values $||P_1^{34}|| \approx 3.028425$ and $||P_2^{34}|| \approx 2.0284207$ correspond to values of ξ_1 and ξ_2 calculated in Example 3.1.

4 Numerical experiments

Three numerical simulations illustrate the algorithms of this paper. More can be found in [Val02, KV03].

4.1 1D beam

To illustrate one-dimensional effects, we study the following beam problem as displayed in Figure 3. We consider the unit square shape $\Omega = (0, 1)^2$ in a $x - y$ coordinate system. The edge 1 is a Dirichlet edge with fixed y coordinate. The intersection point $(0, 0)$ of edges 1 and 2 remains fixed in both coordinates x and y, i.e.,

$$u(0, y) = (0, u_2) \quad \text{for } 0 < y < 1, \quad u(0, 0) = (0, 0).$$

The edges 2 and 3 represent the Neumann edges with zero Neumann condition (tension free surfaces)

$$g(x, 0) = g(x, 1) = (0, 0) \quad \text{for } 0 < x < 1$$

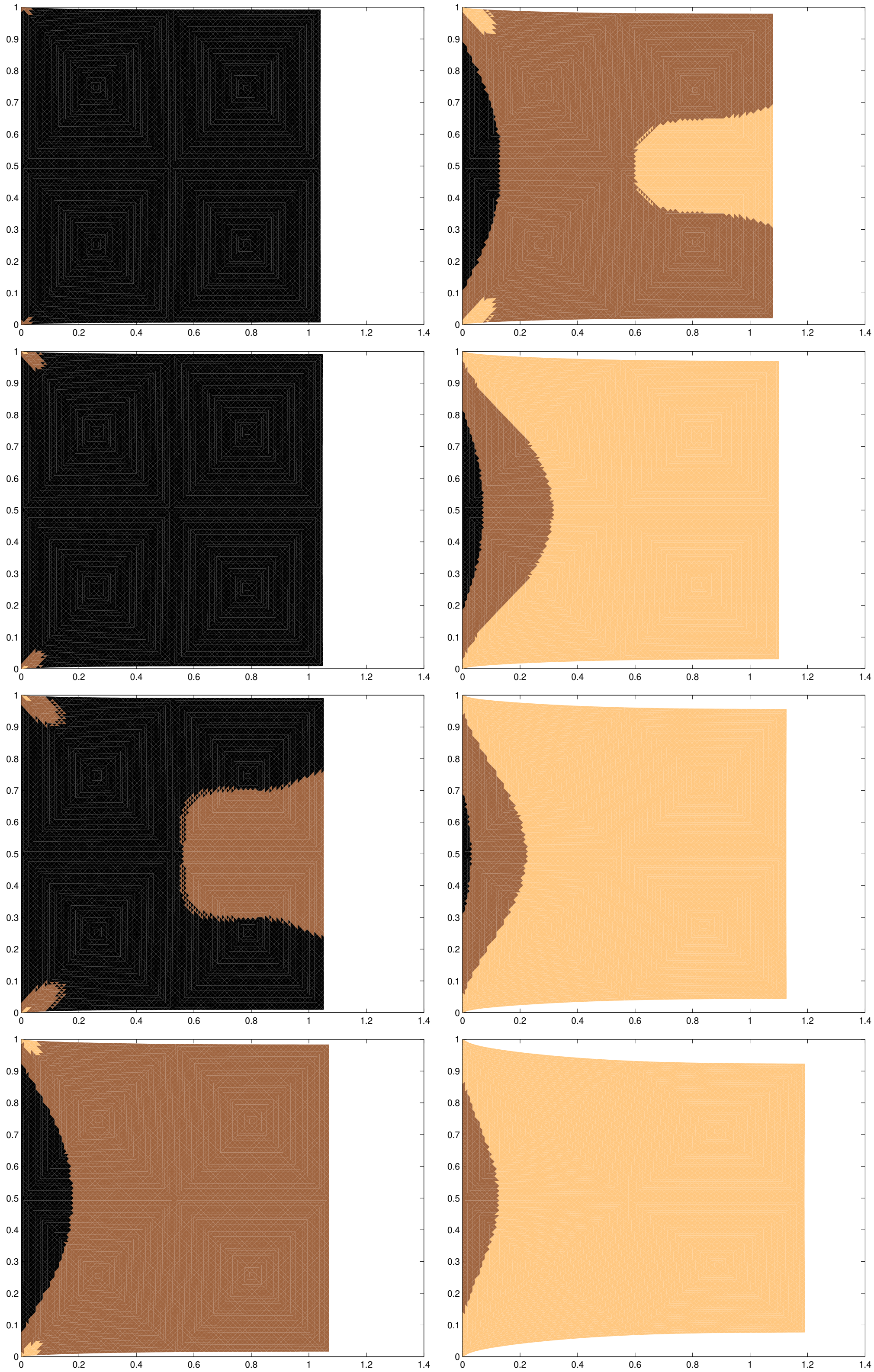

Figure 2: Evolution of elastoplastic zones at discrete times $t = 4.5, 5, 5.5, 6, 6.5, 7,$ $8, 9$ in the numerical experiment with the two-yield 2D beam explained in Subsection 4.2. The black color shows elastic zones, brown and lighter gray color zones in the first and second plastic phase. A corresponding movie can be found in [ani].

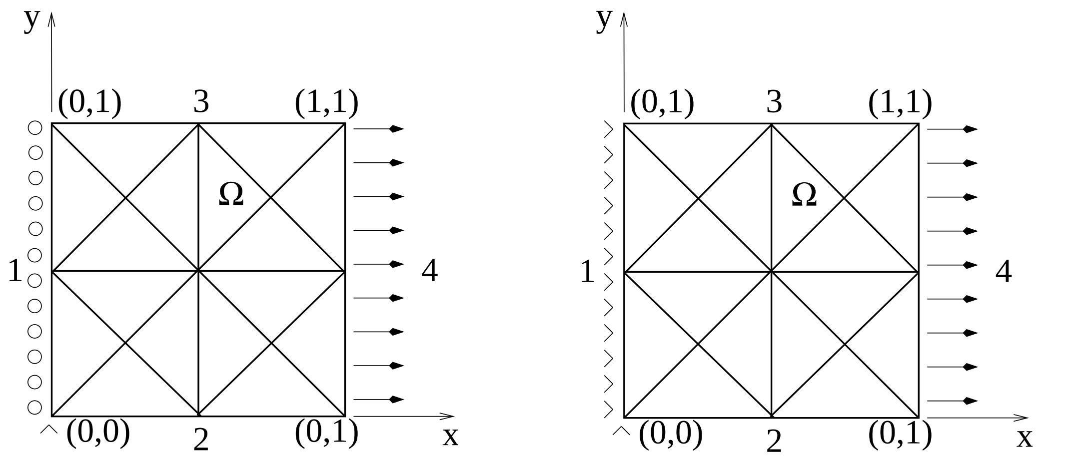

Figure 3: Geometry and coarse mesh $\mathcal{T}_0$ of 1D beam (left) and 2D beam (right).

and the edge 4 is also a Neumann edge with a nonzero Neumann condition representing the constant surface force that deforms the beam in x coordinate

$$g(1,y) = (g_x, 0) \quad \text{for } 0 < y < 1.$$

The deformation of the beam is expected in the form

$$u(x,y) = (u_1,u_2)(x,y) = (x \cdot u_1(1,0), y \cdot u_2(0,1)) \quad \text{for } (x,y) \in \Omega,$$

which implies for the strain tensor

$$\varepsilon(u) = \begin{pmatrix} u_1(1,0) & 0 \\ 0 & u_2(0,1) \end{pmatrix} \quad \text{in } \Omega.$$

Besides that, the Neumann boundary conditions admit the stress tensor

$$\sigma = \begin{pmatrix} g_x & 0 \\ 0 & 0 \end{pmatrix} \quad \text{in } \Omega.$$

There holds Hooke's law in the purely elastic phase (no plasticity), $\sigma = 2\mu\varepsilon + \lambda(\operatorname{tr}\varepsilon)\mathbb{I}$, i.e.,

$$\begin{pmatrix} g_x \\ 0 \\ 0 \end{pmatrix} = \begin{pmatrix} 2\mu+\lambda & \lambda & 0 \\ \lambda & 2\mu+\lambda & 0 \\ 0 & 0 & 2\mu \end{pmatrix} \begin{pmatrix} u_1(1,0) \\ u_2(0,1) \\ 0 \end{pmatrix}.$$

The inverse rule

$$\begin{pmatrix} 2\mu+\lambda & \lambda & 0 \\ \lambda & 2\mu+\lambda & 0 \\ 0 & 0 & 2\mu \end{pmatrix}^{-1} = \begin{pmatrix} \frac{2\mu+\lambda}{4\mu(\mu+\lambda)} & -\frac{\lambda}{4\mu(\mu+\lambda)} & 0 \\ -\frac{\lambda}{4\mu(\mu+\lambda)} & \frac{2\mu+\lambda}{4\mu(\mu+\lambda)} & 0 \\ 0 & 0 & \frac{1}{2\mu} \end{pmatrix}$$

implies that the deformation of the beam can be expressed as

$$u(x,y)(t) = (x\frac{2\mu+\lambda}{4\mu(\mu+\lambda)}, -y\frac{\lambda}{4\mu(\mu+\lambda)})\, g_x(t).$$

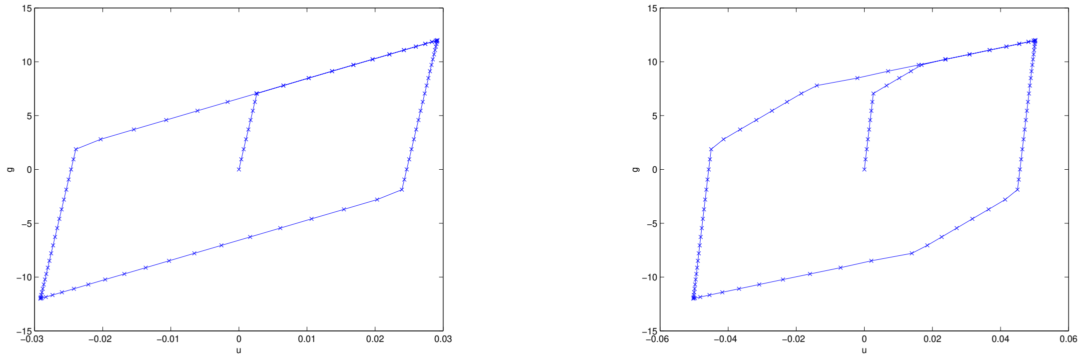

Figure 4: Displayed loading-deformation relation in terms of the uniform surface loading $g_x(t)$ versus the x-displacement of the point $(0,1)$ for problems of the single-yield 1D beam (left) and two-yield 1D beam (right).

The numerical experiment for the hysteresis behavior demonstration was the calculation on the coarse mesh $\mathcal{T}_0$ with 16 elements, discrete times $\{0,\ 0.5,\ 1,\ldots,\ 50\}$, in case of the uniform cyclic surface loading $g_x = 12\sin(t\pi/20)$. In order to compare two different material models, we firstly considered the two-yield material specified by parameters $\mu = 1000, \lambda = 1000, \sigma_1^y = 5, h_1 = 100, \sigma_2^y = 7, h_2 = 50$ and secondly the single-yield material specified by parameters $\mu = 1000, \lambda = 1000, \sigma^y = 5, h = 100$. Figure 4 shows hysteresis curves in terms of the dependence of $g_x(t)$ on the x-displacement $u_x(t)$ of the point $(x = 1, y = 0)$ for the single and two-yield material models.

4.2 2D beam

In order to take two dimensional effects into account, we study a second beam problem. Its geometry is identical to the problem of beam with 1D effects, and the only difference being modified is the Dirichlet boundary condition, see Figure 3. We prescribe the Dirichlet boundary Γ_D in both directions (i.e, the beam is fixed in both directions at Γ_D), i.e.,

$$u(0, y) = (0, 0) \quad \text{for } 0 < y < 1.$$

The first numerical experiment demonstrates two-dimensional hysteresis effects. Material and time parameters, the shape of the mesh and the solver properties are identical to the numerical experiment for the problem of the beam with 1D effects. Figure 5 shows the hysteresis curves for the single and the two-yield material. A comparison of Figure 4 with Figure 5 indicates that two-dimensional deformation effects smooth out the elastoplastic transition.

The second numerical experiment describes an elastoplastic transition during the deformation process. The calculation was performed at discrete times $\{0, 0.5, 1, ...,\ 10\}$, applying the uniform surface loading

$$g_x = t$$

and the same materials as in the first experiment. Figure 2 displays the evolution of elastoplastic zones at chosen discrete times in the deformed configuration. As

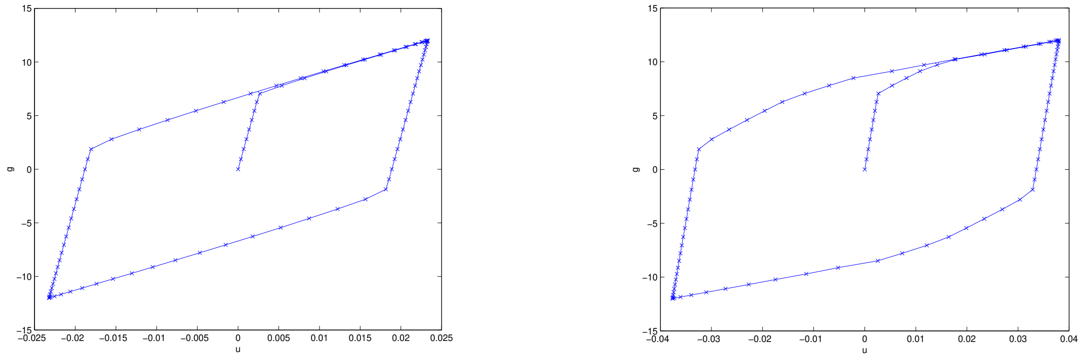

Figure 5: Displayed loading-deformation relation in terms of the uniform surface loading $g_x(t)$ versus the x-displacement of the point $(0, 1)$ for problems of the single-yield beam with 2D effects (left) and two-yield beam with 2D effects (right).

the deformation process starts (at discrete times $t = \{0, 0.5, \ldots, 4.5\}$), the material behaves purely elastically. At discrete time $t = 5.0$ there appear the first plastic zones in corners (where the material is fixed) and also in the right part of the domain Ω (where external forces g act). For the two-yield model there appear the second plastic zones after the discrete time $t = 5.5$, and they develop in the same way as the first plastic zones at the time $t = 5$. For the final discrete time $t = 10$, both material models are in entirely plastic phases. An animation describing the evolution of this process can be downloaded from [ani]. The MATLAB code that was used for the calculation of first two problems can be downloaded from [Val].

4.3 3D crankshaft

Although the paper has been devoted to a two-dimensional notation for the ease of the presentation, the three-dimensional discrete model is straightforward. Hence our final example concerns one time-step crankshaft model [Sch97] shown in Figure 6 (top). The two-yield continuum is specified by material parameters $E = 1, \nu = 0, \sigma_1^y = 1, h_1 = 1, \sigma_2^y = 1.5, h_2 = 1$. The zero Dirichlet condition in the axial direction is set up on the right face of the right central cylinder. The zero Neumann conditions in the normal direction is required on the rest of the cylinder as well as on other two central cylinders. The remaining boundaries are free boundaries with zero Neumann direction. The calculation on the finest uniform mesh with 107776 tetrahedra took 28 minutes and it was performed by an extension of the elasticity package [Kie04]. The package is a part of NETGEN/NGSolve software [Sch] and uses geometrical multigrid preconditioner for the solution of linear system of equations. The resulting elastoplastic phases are displayed in Figure 6 (bottom). The details can be found in [KV03].

Acknowledgments

The authors are pleased to acknowledge support by the German Research Foundation (DFG) through the Graduiertenkolleg 357 “Effiziente Algorithmen und Mehr-

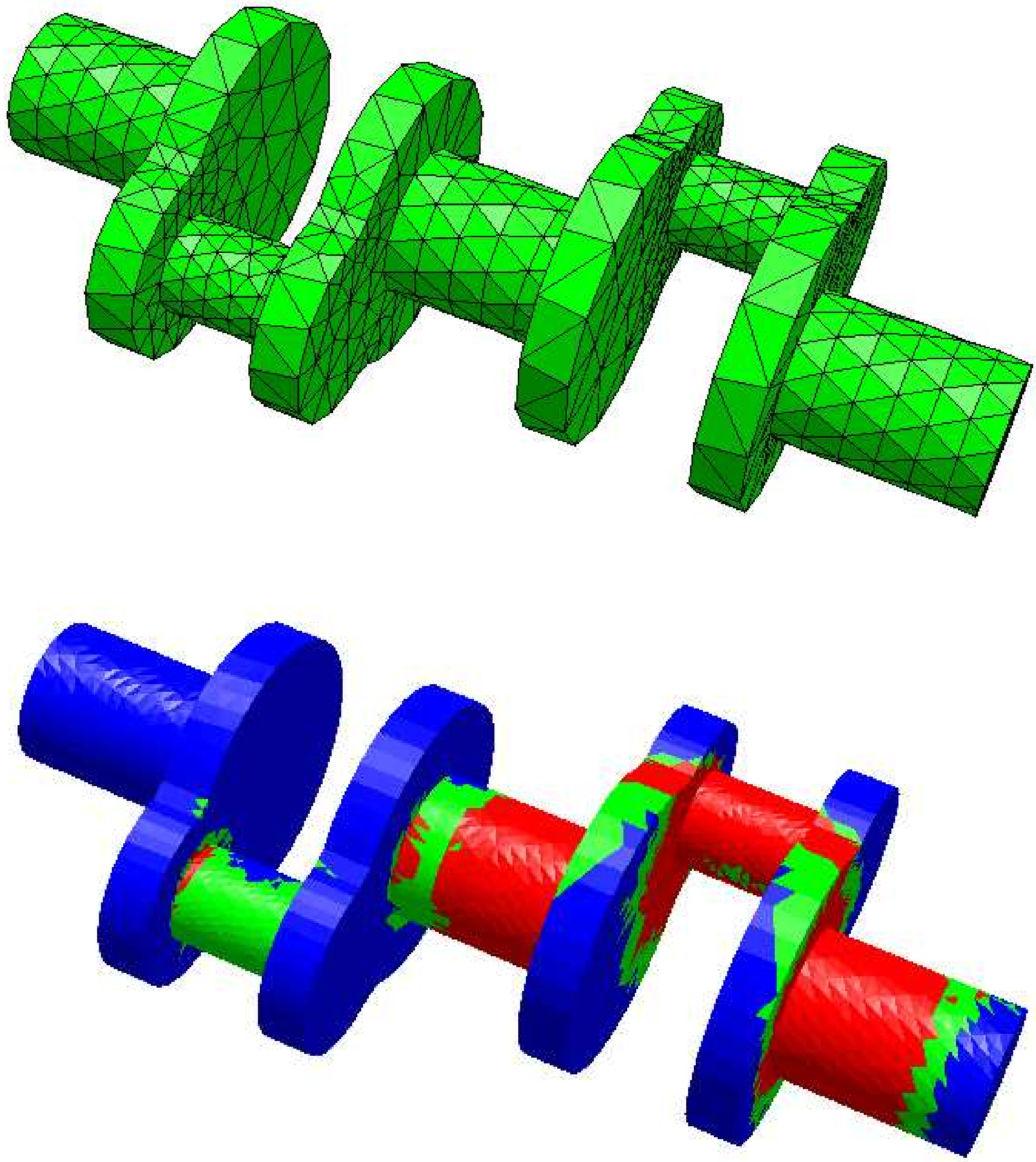

Figure 6: Geometry (top) and elastoplastic zones (bottom) in the numerical experiment with the two-yield crankshaft explained in Subsection 4.3. The blue color shows elastic zones, green and red color zones in the first and second plastic phase. Pictures were generated by NETGEN/NGSOLVE software [Sch].

skalenmethoden" in Kiel, Germany. The third author acknowledges support from the Austrian Science Fund 'Fonds zur Förderung der wissenschaftlichen Forschung (FWF)' for his support under grant SFB F013/F1306 in Linz, Austria. The authors acknowledge software support and advise from J. Alberty, J. Kienesberger and J. Schöberl.

References

[AC00] J. Alberty and C. Carstensen. Numerical analysis of time-depending primal elastoplasticity with hardening. *SIAM J. Numer. Anal.*, 37(4):1271–1294, 2000.

[ACFK02] J. Alberty, C. Carstensen, S. A. Funken, and R. Klose. Matlab implementation of the finite element method in elasticity. *Computing*, 69(3):239–263, 2002.

[ACZ99] J. Alberty, C. Carstensen, and D. Zarrabi. Adaptive numerical analysis in primal elastoplasticity with hardening. *Comput. Methods Appl. Mech. Eng.*, 171(3-4):175–204, 1999.

[ani] http://www.sfb013.uni-linz.ac.at/projects/F1306/beam2d_evolution.gif.

[BCV04] M. Brokate, C. Carstensen, and J. Valdman. A quasi-static boundary value problem in multi-surface elastoplasticity: Part 1 – analysis. *Mathematical Models and Methods in Applied Sciences*, 2004. (accepted).

[Car97] C. Carstensen. Domain decomposition for a non-smooth convex minimalization problems and its application to plasticity. *Numerical Linear Algebra with Applications*, 4(3):177–190, 1997.

[Cia78] P. G. Ciarlet. *The finite element method for elliptic problems.* North-Holland, Amsterdam, 1978.

[Hac85] W. Hackbusch. *Multi-Grid Methods and Applications.* Springer-Verlag Berlin, Heidelberg, 1985.

[HR99] W. Han and B.D. Reddy. *Plasticity: Mathematical Theory and Numerical Analysis.* Springer-Verlag New York, 1999.

[Kie04] J. Kienesberger. Multigrid preconditioned solvers for some elastoplastic problems. In *Proceedings of LSSC 2003*, volume 2907 of *Lecture Notes in Computer Science*, pages 379–386. Springer, 2004.

[KV03] J. Kienesberger and J. Valdman. Multi-yield elastoplastic continuum - modeling and computations. In *ENUMATH Prague 2003*, Lecture Notes in Computer Science. Springer, 2003. (accepted).

[Sch] J. Schöberl. Netgen/Ngsolve - mesh generator/3d finite element solver software package. Download: http://www.hpfem.jku.at/netgen/.

[Sch97] J. Schöberl. Netgen - an advancing front 2d/3d-mesh generator based on abstract rules. *Comput. Visual.Sci*, 1:41–52, 1997.

[Val] J. Valdman. Two-yield elastoplasticity Matlab solver. Download: http://www.sfb013.uni-linz.ac.at/∼jan/solver.zip.

[Val02] J. Valdman. *Mathematical and Numerical Analysis of Elastoplastic Material with Multi-Surface Stress-Strain Relation.* PhD thesis, Christian-Albrechts-Universität zu Kiel, 2002.